

https://doi.org/10.1070/QEL16932

Broadband tunable source of mid-IR laser radiation for photoacoustic spectroscopy

D.B. Kolker, I.V. Sherstov, N.Yu. Kostyukova, A.A. Boyko,
Yu.V. Kistenev, B.N. Nyushkov, K.G. Zenov, A.G. Shadrintseva,
N.N. Tretyakova

Abstract. **Control over volatile products of metabolic processes in human body in exhaled air is a promising method for noninvasive medical diagnostics. The mid-IR range (2–12 μm) is of great interest for diagnostic applications of the exhaled air spectral analysis. Laser optoacoustic spectroscopy is quite attractive for detecting a large set of gaseous substances; however, high-power sources of tunable radiation are required to increase the method sensitivity. We consider the possibility of using a parametric light generator based on a $BaGa_4Se_7$ crystal as a broadband tunable mid-IR laser source for laser optoacoustic spectroscopy.**

Keywords: *volatile organic substances, exhaled air, laser optoacoustic spectroscopy, parametric light generator, chalcogenides.*

1. Introduction. Problem statement

Control over volatile organic substances (VOS's) in exhaled air is a promising approach for the rapid analysis of metabolic processes in human body. In particular, the exacerbation of bronchial asthma is accompanied by an increase in the content of NO, pentane, ammonia, and CO in exhaled air [1–4], and that of ethane in the case of patients with chronic obstructive pulmonary disease [5]. Markers of pneumonia include CO, lipid peroxidation products (LPPs), in particular, propane, butane, hydrogen peroxide, and ammonia [6, 7]. Pulmonary tuberculosis is also accompanied by a release of lipid peroxidation products [8, 9]. Potential markers of lung cancer (LC) in exhaled air samples (EAS's) are alcohols, aldehydes, ketones, and hydrocarbons [10]. In the EAS's of LC patients, an increase in the content of isopropyl alcohol, 2,3-hexanedione, camphor, benzophenone, derivatives of tetroxan, benzene, anthracene, benzoic acid, furan, esters, and also of 3-methyloctane, 3-methylnonane, isoprene, cyclohexane, heptanal , hexanal, and derivatives of heptane, decane, and benzene were observed [11]. Similar VOS's, characteristic of lung cancer, are found in [12]; these are isoprene, 2-methylpentane, pentane, ethylenebenzene, xylene, trimethylbenzene, toluene, benzene, heptane, decane, styrene, octane, and pentamethylheptane. Control measurements [13] revealed a significant decrease in the concentrations of isoprene, acetone, and methanol in EAS's of LC patients, while the concentrations of 2-butanone, benzaldehyde, 2,3-butanedione, 1-propanone, acetophenone, cyclopentene, tetramethylcarbamide, and butyl acetate increased significantly. Diabetes affects not only the acetone content in EAS's, but also the content of CO, CO_2, ethanol, and alkanes [14, 15].

Spectral bands for detecting vibrational modes of the diagnostically significant VOS's mentioned above lie in the range of 3–11 μm [15–18]. Thus, the mid-IR range (2–12 μm) is of great interest for medical applications of the spectroscopic analysis of EAS's.

Various sources can be used to generate tunable laser radiation in the specified range. Gas lasers, such as CO lasers (λ = 2.5–4.2, 4.8–8.3 μm), are common and available; however, the discreteness of wavelength tuning makes it difficult to control a large number of VOS's. Diode lasers usually have a low power (on the order of a few milliwatts in a single-frequency regime) and a small range ($\sim$0.1 μm) of continuous wavelength tuning. Quantum-cascade lasers also have a relatively small tuning range (less than 1 μm) and are expensive.

Laser photoacoustic spectroscopy (LPAS) is generally quite attractive for detecting a large set of gaseous substances because it possesses a large dynamic range, low detection limit, sufficient selectivity, and requires a small amount of gas sample for analysis. In selecting a radiation source for LPAS, it is necessary to take into account that the acoustic signal is proportional to the energy absorbed by the gas sample. To obtain the required average power of IR radiation, along with gas lasers, optical parametric oscillators (OPOs) can be used, which also provide continuous broadband tuning [19].

Chuchumishev et al. [20] describe a tunable optical parametric amplifier of the mid-IR range, in which a periodically polarised structure based on stoichiometric lithium tantalate (PPSLT) is used as a nonlinear element. Pumping was performed by a system based on a Nd laser, the pulse duration was 800 ps, the repetition rate was 0.5 kHz, and the energy was up to 40 mJ. The idler wave spectral tuning in the range of 3–3.5 μm was conducted at the temperature change of the

D.B. Kolker Institute of Laser Physics, Siberian Branch, Russian Academy of Sciences, prosp. Akad. Lavrent'yeva 15b, 630090 Novosibirsk, Russia; Novosibirsk State University, ul. Pirogova 1, 630090 Novosibirsk, Russia; Tomsk State University, prosp. Lenina 36, 634050 Tomsk, Russia; Novosibirsk State Technical University, prosp. K. Marksa 20, 630072 Novosibirsk, Russia;
I.V. Sherstov, N.Yu. Kostyukova, A.A. Boyko, B.N. Nyushkov Institute of Laser Physics, Siberian Branch of the Russian Academy of Sciences, prosp. Akad. Lavrent'yeva 15b, 630090 Novosibirsk, Russia; Novosibirsk State University, ul. Pirogova 1, 630090 Novosibirsk, Russia;
Yu.V. Kistenev Tomsk State University, prosp. Lenina 36, 634050 Tomsk, Russia; Institute of Strength Physics and Materials Science, Siberian Branch, Russian Academy of Sciences, prosp. Akademicheskii 2/4, 634055 Tomsk, Russia; e-mail: yuk@iao.ru;
K.G. Zenov, A.G. Shadrintseva, N.N. Tretyakova 'Special Technologies' Ltd., ul. Zelenaya gorka 1/3, 630053 Novosibirsk, Russia

Received 15 September 2018; revision received 3 December 2018
Kvantovaya Elektronika **49** (1) 29–34 (2019)
Translated by M.A. Monastyrskiy

nonlinear element. The system provided the pulse generation at the idler wave frequency, with an energy of 4.1 mJ and a duration of 600 ps.

An OPO capable of simultaneous generation of radiation at two wavelengths (3295 and 3469 nm) was presented in paper [21]. To reduce the signal wave loss, a single-cavity OPO with coaxially arranged nonlinear KTA and KTP crystals was used. Various polarisation components of Nd:YAG laser radiation could separately pump nonlinear crystals, thus implementing a parallel OPO scheme. Thus, the maximum average power was 1.01 and 0.81 W, the peak pulse power was 23.3 and 18.7 kW at wavelengths of 3295 and 3469 nm, respectively, with a pulse duration of 6.2 ns.

A $KTiOAsO_4$ crystal pumped by a Nd:YAG laser was used as a nonlinear element to design an OPO with wavelength tuning in the range of 3–4 μm; the pulse energy was no less than 6 mJ, the pulse repetition rate was 10 Hz, and the generation line width was 1–5 cm^{-1} [22, 23].

In mid-IR OPOs pumped by radiation from a *Q*-switched Tm:YAP laser (λ_p = 1.94 μm) [24], latest-generation ZGP and CSP crystals having low absorption at the pump wavelength were used for parametric radiation conversion. Various two-cavity OPO configurations, including those with single- and double-pass pumping, were investigated. Oscillations were implemented in the range of 3.6–4.2 μm. In the case of double-pass pumping, the maximum radiation power reached 2.3 and 2.5 W with an optical conversion efficiency of 58% and 64% for ZGP and CSP crystals, respectively.

In work [25], an OPO with double-pass pumping based on periodic MgO:PPLN structures is described. A small-size nanosecond Nd:YLF laser (λ_p = 1.053 μm) served as a pump source, the pump pulse duration was 5–7 ns at a maximum pulse energy of 300 μJ and a repetition rate of 1–7 kHz. The OPO threshold of MgO:PPLN-based OPO was varied in the range of 11–28 μJ with the wavelength range of 2.1–4.3 μm. The efficiency of pump energy conversion into the idler wave energy decreased from 8.6% to 2.5% in the range of 2–4.3 μm. In the 4.2 μm region, the generation threshold constituted 36 μJ, while that in the 4.7 μm region it was 49 μJ. The conversion efficiency in the spectral range 4.2–4.7 μm was 3.3%–0.4%.

There are a limited number of nonlinear crystals for parametric conversion of 1 μm radiation to the spectrl range of 3–30 μm. Vodopyanov et al. [26] presented a parametric light generator based on $AgGaS_2$ (AGS) with laser pumping (λ_p = 1 μm) providing the idler wave generation up to 11.3 μm. $HgGa_2S_4$ (HGS) crystals have high energy characteristics, i.e. a pulse energy up to 3 mJ at a wavelength of 6.3 μm was obtained [27]; however, the technology for growing HGS crystals of required size is extremely complex. $Cd_xHg_{1-x}Ga_2S_4$ solid solutions are also used for OPOs, but the control over their composition represents a complex problem. Chalcopyrite (CSP) crystals have high nonlinearity but low radiation resistance, and their transparency range is limited to 6.5 μm [28].

Nonlinear $ZnGeP_2$ (ZGP) and $CdSiP_2$ (CSP) crystals as well as orientation-patterned gallium arsenide [(OP)-GaAs] and gallium phosphide [(OP)-GaP] crystals are promising for the development of the mid-IR range OPOs. With the use of (OP)-GaP crystals as a nonlinear medium, the generation of continuous radiation with tuning in the range of 4608–4694 nm was implemented. In particular, for a 40 mm long crystal, a power over 30 mW was obtained at the OPO output within virtually entire (more than 95%) tuning range at a maximum power up to 43 mW [29].

Based on a (OP)-GaAs structure pumped by picosecond laser source radiation (λ_p = 1.952 μm), Fu et al. [30] designed an OPO with tuning ranges of 2552–2960 nm (signal wave) and 5733–8305 nm (idler wave). The maximum pulse energy was 0.40 μJ (for a signal wave at a wavelength of 2942 nm) and 0.16 μJ (an idler wave, 5800 nm) with an overall conversion efficiency of 22.4%. The duration of generated pulses was 36 ps.

Boyko et al. [31] investigated the intracavity differential frequency generation (DFG) in the OPO cascade scheme. An OPO based on the PPKTP periodic structure was used as the first cascade. In the second cascade, the (OP)-GaAs structure was used to implement DFG for the signal and idler waves of the first OPO cascade. The first cascade was pumped by a nanosecond Nd:YAG laser ($\lambda_p \approx$ 1 μm). The DFG wide tuning range of 7–9.2 μm at an average power of ~10 mW (repetition rate of 1–3 kHz) was demonstrated.

Earlier, we have presented a 'LaserBreeze' photoacoustic laser analyser, which employed a combined OPO based on nonlinear fan-out MgO:PPLN and HGS crystals as a radiation source with a tuning range of 2.7–10.6 μm [32]. The recording time of the LPAS absorption spectrum was 5–8 min, since the OPO radiation wavelength tuning was performed by rotating the HGS crystal and displacing the fan-out MgO:PPLN structure along the *Y* axis relative to the OPO resonator axis. An additional disadvantage of such a system is a complex nonlinear dependence of the tunable wavelength in scanning the entire spectral range, which complicates its control during the scanning process.

Recently, $BaGa_4S_7$ (BGS) and $BaGa_4Se_7$ (BGSe) chalcogenide crystals have appeared, which are promising for the mid-IR range; the latter crystal has a transparency range of 0.47–18 μm, which potentially allows for the wavelength tuning up to 18 μm [28].

In this work, we consider the possibility of using an OPO based on the $BaGa_4Se_7$ crystal for LPAS.

2. Experimental implementation of an OPO based on the $BaGa_4Se_7$ crystal

A BGSe crystal is biaxial and belongs to the symmetry class *m* of monoclinic syngony. In this case, the crystal's dielectric axes *X* and *Z* coincide with the corresponding crystallographic axes *b* and *c* [33–37].

An optical parametric oscillator based on a BGSe nonlinear crystal was first implemented in [38]. The pump source was a *Q*-switched Ho:YAG laser (λ_p = 2.09 μm). A crystal measuring 6 × 6 × 30 μm and oriented in the *Y* plane (θ = 40.8°, φ = 0°) was used to implement the first type interaction (o–ee) in the *XZ* plane. The tuning range was 3–5 μm, which did not exceed the upper limit (5 μm) for oxide ferroelectrics; the optical efficiency reached 7% (~1.4 mJ at a pump energy of 20 mJ).

Kostyukova et al. [28] described the OPO implementation on a BGSe crystal pumped by a Nd:YAG laser (λ_p = 1064 nm). The BGSe crystal was cut out with cut angles θ = 46°, φ = 0° and had a size of 10.33 × 11.95 × 14.57 mm^3. The use of a high-power Nd:YAG laser (pump energy E_p up to 250 mJ, pulse duration τ_p = 8 ns, repetition rate f_p = 10 Hz) allowed us to obtain an idler wave energy of 3.7 mJ for a wavelength of 7.2 μm at E_p = 63 mJ without significant saturation at a quantum efficiency of ~40% (the output energy limitation was stipulated not by the BGSe crystal destruction

threshold, but by a possible damage to the rear reflecting mirror of the OPO resonator).

2.1. Experimental setup

The block diagram of the experimental setup is shown in Fig. 1. A *Q*-switched diode-pumped Nd:YLF laser (TECH-1053-N, Laser-Compact, Russia) was used as a pump source for the BGSe OPO. Its parameters were as follows: pump wavelength λ_p = 1.053 μm, pulse duration τ_p = 16 ns, pulse repetition rate f_p = 100 Hz, and radiation line width $\Delta\nu_p \approx$ 1 cm^{-1} (30 GHz). The maximum pump pulse energy did not exceed 1.3 mJ, and the beam quality parameters were $M_x^2 = M_y^2 = 1.3$. Note that, in contrast to work [28], the pump laser had not only a shorter wavelength (1.053 μm), but also a much lower (about 50 times) pulse energy [39].

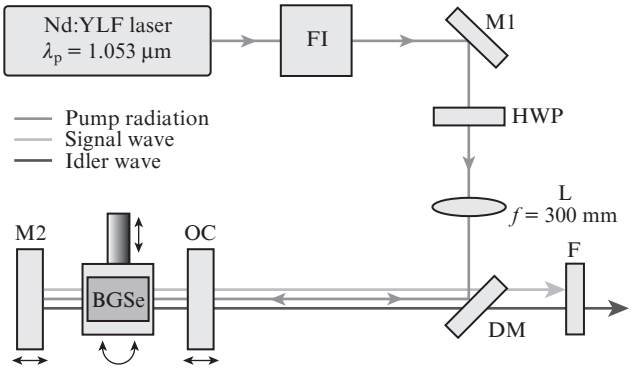

Figure 1. OPO block diagram:
(FI) Faraday isolator; (M1) mirror; (HWP) half-wave plate; (L) lens; (DM) dichroic mirror; (OC) output coupler made of ZnSe for radiation input and output into and out of the OPO resonator; (M2) gold-coated reflective mirror; (F) interference filters.

A single-resonant OPO resonator was formed by two mirrors, the transmittance and reflectance of which provided the possibility of operation with double-pass pumping. In this scheme, the resonance took place only for the signal wave; optical feedback for the pump laser was suppressed by a Faraday insulator. A half-wave plate was rotating the polarisation direction of pump laser radiation vertically relative to the *XZ* plane of the BGSe crystal in order to meet the first type (o–ee) phase-matching condition. Due to the pump pulse energy smallness, the pump beam diameter to reach the threshold of parametric generation was reduced using a lens with a focal length f = 300 mm (BK7 optical glass) to a spot with sizes $2w_x$ = 0.42 mm and $2w_y$ = 0.42 mm.

Pump laser radiation was directed to the OPO resonator by a dichroic mirror (DM) from ZnSe at an angle of 45°.The mirror had a high reflectance (~97% on average at normal incidence) within a wavelength range of 1.0–1.1 μm and a high transmittance (~90%) within a wavelength range of 1.15–10 μm. Several combinations of interference filters (F) were used to ensure the most efficient output of the idler wave radiation from the OPO, and also filtering of the pump radiation partially passed through the DM folding mirror.

The ZnSe OC provided the input and output of radiation. The gold-coated rear mirror of the OPO resonator had a high (~98%) reflectance over the entire operating range. The resonator length was chosen as small as possible ($L_{cav} \geqslant 18$ mm) to increase the number of signal wave bypasses and decrease the pump energy value to reach the parametric generation threshold. The input concave mirror (curvature radius R = 1000 mm) reduced the signal wave divergence. The mirror transmittance T at λ_p = 1.053 μm was 93%; the reflectance R_s was about 90% in the wavelength range 1.28–1.8 μm and gradually decreased to about 60% in the wavelength range 1.8–2.1 μm. The average value of the coefficient T in the range 2.28–11 μm (for idler wave) was 75%.

We used a 3 × 7 × 11.8 mm $BaGa_4Se_7$ crystal (Fig. 2) grown at the Kuban State University (Russia) by Bridgman–Stockbarger method. The crystal is designated to implement the first type phase-matching condition ($\theta = 45°$, $\varphi = 0°$), the direction of pump radiation polarisation is chosen along the side of 3 mm (dielectric axis direction), the direction of signal (idler) wave polarisation lies in the *XZ* plane (upper or lower crystal faces in Fig. 2). To provide a broadband range of OPO tuning by crystal rotation, a wider transverse aperture of 7 mm was used.

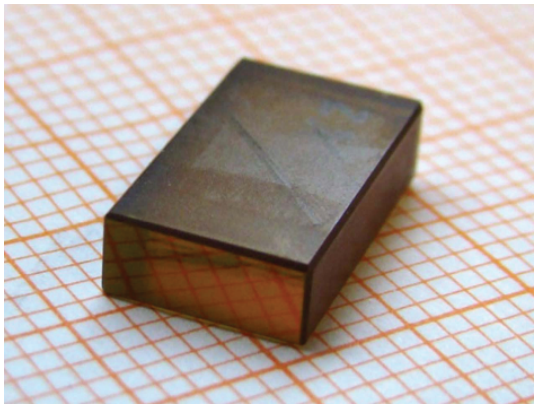

Figure 2. (Colour online) Photograph of the BGSe crystal. The dark yellow shade is due to certain absorption at the origin of the visible part of the spectrum.

The BGSe crystal was placed into a copper holder with a thermostat at a constant temperature (40 ± 0.1 °C) that was maintained using a Peltier element. A single-layer antireflection coating centred at a wavelength of ~1.5 μm was deposited onto the crystal's working faces, which provided a high crystal transmittance (more than 85%) in the range of 1–2 μm (Fig. 3). In the mid-IR range of 5–11 μm, the transmittance constituted ~72%, which was greater than that of uncoated crystals.

To implement the wavelength tuning, the holder with BGSe crystal was placed on a STANDA 8-MR-191-30 motorised rotation platform. The phase-matching angle was determined by recalculation of the measured crystal setting angle (relative to the normal pump beam incidence) into the value of internal crystal angle in accordance with the Snell law.

To shift the crystal in the direction perpendicular to the resonator optical axis, an additional linear translation stage was also used (STANDA 8MT173-20). By using a computer-connected controller, the crystal rotation angle θ together with its linear offset relative to the resonator optical axis was monitored. To ensure the maximum range of wavelength tuning (the BGSe crystal orientation angle θ = 45° corresponds to the idler wavelength $\lambda_i \approx 8$ μm), the distance between the resonator-forming M2 and OC was increased.

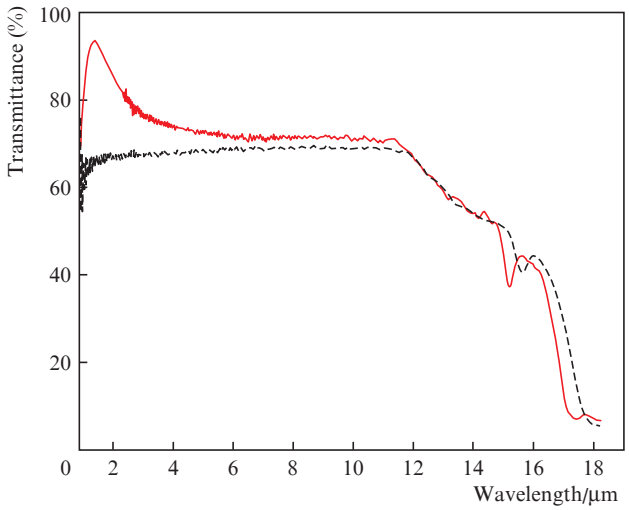

Figure 3. Transmittance spectra of the BGSe crystal sample with a length of 12.8 mm for nonpolarised radiation before (dashed curve) and after (solid curve) deposition of an antireflective coating providing greater transmittance at the pump wavelength and in the signal wavelength range (1.17–2.02 μm).

2.2. BGSe-based OPO tuning range

For a BGSe-based OPO, the experimental dependence of the idler energy on the wavelength was measured after the OC (Fig. 4). A HighFinesse (LSA L IR) wavelength meter was used for wavelength determination in the range of 2.6–10.4 μm. The idler wavelength value was obtained by calculation using the energy conservation law

$$(\lambda_p)^{-1} = (\lambda_s)^{-1} + (\lambda_i)^{-1}.$$

The energy of the idler wave was measured with a pyroelectric detector (OPHIR, VEGA PE10-C). The use of filters ensured effective radiation blocking only for wavelengths below 1.683 μm; in this regard, in the wavelength range from about 2.2 μm (near the $2\lambda_p$ degeneration point) to 2.6 μm, the idler wave energy could not be properly measured due to high energy level of the signal wave. Therefore, the $E_i(\lambda)$ dependence is shown for wavelengths greater than 2.6 μm.

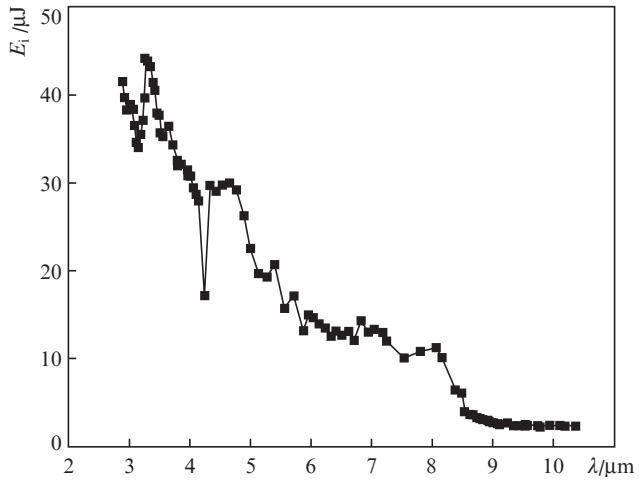

Figure 4. Idler energy vs. idler wavelength.

The idler wavelength tuning implemented on a single BGSe crystal was observed in the range 2.2–10.5 μm, which exceeds the tuning range 5.6–10.8 μm obtained in Ref. [40], in which two HGS crystals with orientation angles $\theta = 47°$ and 60° were used for lasing. Despite the fact that the nonlinearity coefficient $\chi^{(2)}$ in HGS is 4 times greater than that in BGSe, the idler wave output energy in the OPO based on the BGSe crystal was 4–5 times higher than that in the OPO based on the HGS crystal; in this case, the maximum pulse energy constituted 45 μJ at a wavelength of ~3.3 μm and 14 μJ at a wavelength of ~8 μm (for the HGS crystal-based OPO, the energy E_i was less than 8 μJ over the entire tuning range of 4.2–10.8 μm). Such a wide tuning range on a single BGSe crystal demonstrates its advantages compared to the HGS crystal.

A general tendency to reducing the conversion efficiency (see Fig. 4) is stipulated by the inversely proportional dependence of parametric amplification on λ_i. The output energy peak value (E_i = 45 μJ) near 3.3 μm corresponds to a high optical system efficiency, since the input mirror reflectance R_s = 95% in the range 1.4–1.62 μm (λ_s = 1.55 μm).

A sharp drop in E_i at a wavelength of 4.2 μm and within the 5.5–6 μm region is obviously due to the radiation absorption by atmospheric gases (CO_2 and water vapour). A small increase in E_i near 8.1 μm corresponds to the usually observed increase in amplification of similar nanosecond OPOs, when the crystal is located normally to the linear resonator axis [28, 37], thus resulting in the so-called reference resonator effect stipulated by the presence of the plane-parallel faces of optical elements having an antireflective coating in this range. Note that, because of the 10 times smaller pump beam diameter, the idler wave energy we obtained is lower compared to that in work [28].

The pulse energy dependence in the range of 9.2–10.4 μm is due to the fact that, in this range, the input mirror reflectance for the signal wave drops sharply from 50% to 20%. The reduction in amplification for the signal wave in the resonator probably replaces the parametric generation process with the parametric amplification process in the specified range.

Figure 5 shows the the angle tuning OPO curve for signal and idler waves in the IR range. It can be seen that the idler wavelength can be tuned virtually from the degeneration point ($\lambda_s = \lambda_i = 2\lambda_p$ = 2.106 μm) to 10.5 μm. Herewith, in the near-IR range, the idler wavelength was measured directly (points in Fig. 5), while, in the other part of the IR range, the dependence was constructed by measuring the signal wavelength (squares in Fig. 5) with subsequent recalculation into the idler wavelength using the energy conservation law.

Because of the relatively low radiation energy from the Nd:YLF laser (E_p < 1 mJ at the OPO input mirror) and smaller value of parametric amplification that leads to a higher lasing threshold, we were unable to attain the same value of maximum wavelength retuning (17 μm) that was given in work [28], obtained for a similar BGSe crystal sample, but with much more powerful pump radiation from the Nd:YAG laser (E_p > 100 mJ).

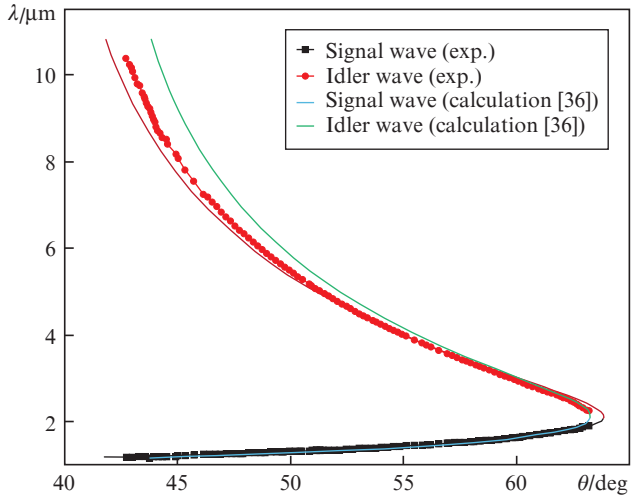

Figure 5. Dependence of the wavelength on the phase-matching angle in the BGSe crystal pumping by radiation from the Nd : YLF laser (λ_p = 1.053 μm) for the first type interaction (o–ee).

3. Conclusions

The work presents the results of experimental study on the BGSe-based OPO pumped by a *Q*-switched Nd : YLF laser (λ_p = 1.053 μm). The first type of interaction (o-ee) in the *Y* plane was used. The BGSe-based OPO threshold was 0.25 mJ. It was found that the BGSe damage threshold was estmated to be ~ 2.04 J cm^{-2} at a pulse repetition rate of 100 Hz. In the experiment, the idler wavelength tuning range 2.6–10.4 μm was implemented.

The use of the $BaGa_4Se_7$ crystal-based OPO as a radiation source in the 'LaserBreeze' laser photoacoustic spectrometer makes it possible to abandon the cumbersome scheme of a combined OPO [32], in which switching of two OPO blocks occurs in the process of wavelength scanning: one of them is based on the fan-out PPLN, while the other one, on a tandem of two HGS crystals providing the wavelength tuning in the range 2.7–10.6 μm. Since the entire tuning range (2.6–10.8 μm) in the OPO presented is realised only at the expense of angular tuning of a single nonlinear BGSe crystal, the spectrometer optical scheme turns out much simpler compared to that employed in 'LaserBreeze', which leads to more reliable radiation wavelength control in the process of sample spectral scanning, a decrease in scanning time, and an increase in stability.

References

1. Jatakanon A., Lim S., Kharitonov S.A., et al. *Thorax*, **53**, 91 (1998).
2. Kharitonov S.A., Barnes P.J. *Am. J. Respir. Crit. Care Med.*, **163**, 1693 (2001).
3. Selivanova P.A., Starovoytova E.A., Kulikov E.S., Krasnobaeva L.A. *Bull. Sib. Med.*, **4**, 15 (2011).
4. Horvath I., Donnelly L.E., Kiss A., et al. *Thorax*, **53**, 668 (1998).
5. Paredi P., Kharitonov S.A., Leak D., Ward S., Cramer D., Barnes P.J. *Am. J. Respir. Crit. Care Med.*, **162**, 369 (2000).
6. Alyakrinskaya M.D., Komar S.I. *Izv. Chelyab. Nauchn. Tsentra*, **1** (35), 179 (2007).
7. Lechner M., Rieder J. *Current Med. Chem.*, **14**, 987 (2007).
8. Phillips M., Ring Erickson G.A., Greenberg J., La Bombardi V., Munawar M.I., Tietje O. *Tuberculosis*, **87**, 44 (2007).
9. Kwiatkowska S., Szkudlarek U., Łuczyn´ska M., Nowak D., Zieba M. *Respiratory Medicine*, **101**, 574 (2007).
10. Cao W. *Clin. Chem.*, **5**, 800 (2006).
11. Altorki N., Phillips M., Nasser A. *Clin. Chim. Acta*, **2**, 76 (2008).
12. Carbognani P., Poli D. *Respir. Res.*, **6**, 71 (2005).
13. Bajtarevic A., Ager C., Pienz M., Klieber M., Schwarz K., Ligor M., Ligor T., Filipiak W., Denz H., Fiegl M., Hilbe W., Weiss W., Lukas P., Jamnig H., Hackl M., Haidenberger A., et al. *BMC Cancer*, **9**, 348 (2009).
14. Turner C., Walton C., Hoashi S., Evans M. *J. Breath Res.*, **3**, 046004 (2009).
15. Greiter M.B., Keck L., Siegmund T., Hoeschen C., Oeh U., Paretzke H.G. *Diabetes Technology & Therapeutics*, **12**, 455 (2010).
16. Kistenev Y.V., Bukreeva E.B., Bulanova A.A., Kuzmin D.A., Karapuzikov A.I., Kostyukova N.Y., Starikova M.K., Boyko A.A., Kolker D.B., Zenov K.G., Karapuzikov A.A. *J. Biomed. Opt.*, **20**, 065001 (2015).
17. Stacewicz T., Bielecki Z., Wojtas J., Magryta P., Mikolajczyk J., Szabra D. *Opto-Electron. Rev.*, **24**, 82 (2016).
18. Wang C., Sahay P. *Sensors*, **9**, 8230 (2009).
19. Li J., Chen W., Yu B. *Appl. Spectr. Rev.*, **46**, 440 (2011).
20. Chuchumishev D., Trifonov A., Oreshkov B., Xu X., Buchvarov I. *Appl. Phys. B*, **124**, 147 (2018).
21. Huang H., Wang S., Liu X., Shen D. *Infrared Physics and Technology*, **93**, 91 (2018).
22. Matvienko G.G., Romanovskii O.A., Sadovnikov S.A., Sukhanov A.Ya., Kharchenko O.V., Yakovlev S.V. *J. Opt. Technol.*, **84**, 408 (2017).
23. Romanovskii O.A., Sadovnikov S.A., Kharchenko O.V., Yakovlev S.V. *J. Appl. Spectr.*, **85**, 457 (2018).
24. Cole B., Goldberg L., Chinn S., Zawilski K.T., Pomeranz L.A., Schunemann P.G., McCarthy J.C., Hopkins F.K. *Proc. SPIE, Solid State Lasers XXVII: Technology and Devices*, **10511**, 105110H (2018).
25. Kolker D.B., Pustovalova R.V., Starikova M.K., Karapuzikov A.I., Karapuzikov A.A., Kuznetsov O.M., Kistenev Yu.V. *Prib. Tekn. Eksp.*, **2**, 124 (2012).
26. Vodopyanov K.I., Maffetone J.P., Zwieback I., Ruderman W. *Appl. Phys. Lett.*, **75**, 1204 (1999).
27. Esteban-Martin A., Marchev G., Badikov V., Panyutin V., Petrov V., Shevyrdyaeva G., Badikov D., Starikova M., Sheina S., Fintisova A., Tyazhev A. *Laser Photon. Rev.*, **7**, L89 (2013).
28. Kostyukova N., Boyko A., Badikov V., Badikov D., Shevyrdyaeva G., Panyutin V., Marchev G., Kolker D., Petrov V. *Opt. Lett.*, **41**, 3667 (2016).
29. Devi K., Padhye A., Schunemann P.G., Ebrahim-Zadeh M. *Opt. Lett.*, **43**, 2284 (2018).
30. Fu Q., Xu L., Liang S., Shepherd D.P., Richardson D.J., Alam S. *IEEE J. Sel. Top. Quantum Electron.*, **24**, 5100706 (2018).
31. Boyko A.A., Schunemann P.G., Guha S., Kostyukova N.Y., Kolker D.B., Panyutin V.L., Marchev G.M., Pasiskevicius V., Zukauskas A., Mayorov F., Petrov V. *Opt. Mater. Express*, **8**, 549 (2018).
32. Karapuzikov A.A., Sherstov I.V., Karapuzikov A.I., Shtyrov M.Y., Dukhovnikova N.Y., Zenov K.G., Boyko A.A., Starikova M.K., Tikhonyuk I.I., Miroshnichenko I.B., Miroshnichenko M.B., Kolker D.B., Myakishev Y.B., Lokonov V.N., Kistenev Y.V., Kuzmin D.D. *Phys. Wave Phenomena*, **22**, 189 (2014).
33. Kolker D.B., Sherstov I.V., Kostyukova N.Yu., Boyko A.A., Zenov K.G., Pustovalova R.V. *Quantum Electron.*, **47**, 14 (2017) [*Kvantovaya Elektron.*, **47**, 14 (2017)].
34. Badikov V., Badikov D., Shevyrdyaeva G., Tyazhev A., Marchev G., Panyutin V., Petrov V., Kwasniewski A. *Phys. Status Solidi RRL*, **5**, 31 (2011).
35. Yao J., Yin W., Feng K., Li X., Mei D., Lu Q., Ni Y., Zhang Z., Hu Z., Wu Y. *J. Cryst. Growth*, **346**, 1 (2012).
36. Boursier E., Seconds P., Ménaert B., Badikov V., Panyutin V., Badikov D., Petrov V., Boulanger B. *Opt. Lett.*, **41**, 2731 (2016).

37. Tyazhev A., Kolker D., Marchev G., Badikov V., Badikov D., Shevyrdyaeva G., Panyutin V., Petrov V. *Opt. Lett.*, **37**, 4146 (2012).
38. Yuan J.H., Li C., Yao B.Q., Yao J.Y., Duan X.M., Li Y.Y., Shen Y.J., Wu Y.C., Cui Z., Dai T.Y. *Opt. Express*, **24**, 6083 (2016).
39. Kolker D.B., Kostyukova N.Yu., Boyko A.A., Badikov V.V., Badikov D.V., Shadrintseva A.G., Tretyakova N.N., Zenov K.G., Karapuzikov A.A., Zondy J.-J. *J. Phys. Commun.*, **2**, 035039 (2018).
40. Kostyukova N.Y., Kolker D.B., Zenov K.G., Boyko A.A., Starikova M.K., Sherstov I.V., Karapuzikov A.A. *Laser Phys. Lett.*, **12**, 095401 (2015).